ISSN 2321-807X

Adsorption of Hexavalent Chromium and phenol onto Bentonite Modified With HexaDecylTriMethylAmmonium Bromide (HDTMABr)

My. S. Slimani, H. Ahlafi*, H. Moussout, F. Boukhlifi, O. Zegaoui

Equipe : Matériaux et Catalyse Appliqués, Laboratoire de Chimie et Biologie Appliquées à l'Environnement, Département de chimie, Faculté des Sciences : B.P.11201, Zitoune, Université Moulay Ismaîl, Meknès, Morocco

Corresponding author : E-mail : hahlafi@yahoo.fr

ABSTRACT

The efficiencies of Hexadecyltrimethylammonium bromide (HDTMABr) modified bentonite (HDTMABt) for phenol and chromium removal from aqueous solutions were studied in batch experiments at pH = 9 and pH = 2 values, respectively. FTIR, SEM, XRD and BET analyses indicated that the HDTMABr molecules were intercalated in the interlayer and at the external surface of initially Na-bentonite (NaBt). Adsorption experiments showed that the HDTMABt was more efficient than the initial NaBt for the removal of phenol and chromium, simultaneously, the extent of the enhancement differed among these pollutants depending on their affinity towards these samples. The kinetic study revealed a rapid adsorption onto HDTMABt of the pollutants during the initial stage (t_{eq} < 1h). The pseudo-second-order equation fitted well to the experimental data. Phenol adsorption on NaBt and HDTMABt could be described by a linear Freundlich equation while Langmuir and Freundlich models were the most suitable for Cr(VI) adsorption on both samples.

Keywords

Bentonite; Organoclays; Hexavalent chromium; phenol; Adsorption; Hexadecyltrimethylammoniumbromide.

.

Council for Innovative Research

Peer Review Research Publishing System

Journal: Journal of Advances in Chemistry

Vol. 8, No. 2

editor@cirjac.com

www.jac.cirworld.com, member.cirworld.com

ISSN 2321-807X

1. INTRODUCTION

In recent years, the protection of the natural environment, especially the quality of water, has become a major worldwide concern. Water pollution is a continuing threat to humans and their environment due to the abusive use and uncontrolled release of toxic substances. A head of the latters are phenol and hexavalent chromium which have been considered major organic and inorganic primary pollutants worldwide because to numerous health problems arising from groundwater contamination [1, 2, 3]. The augmentation of phenol and chromium concentrations in soils, water and sediments, exceeding the accepted standard values may be the results not only human activities but also natural anomalies.

To remedy this problem, several methods have been developed to remove these pollutants from aqueous solutions such as precipitation/coagulation, ion exchange, membrane processing [4, 5]. However, some of these methods have their own strengths and limitations, and are found to be expensive, less effective or generate additional by-products. Several researches have shown that adsorption process, especially when combined with low cost adsorbents like clay, biomass and biosorbant materials, was considered the best at removing inorganic and organic pollutants from the water or wastewater treatment because of convenience, simplicity and lower operating cost [6 - 11]. For example, adsorption on activated carbon is well known in the process of the removal of phenol and Cr(VI) and other pollutants, since the activated carbon has a high adsorption capacity; however, its high cost limits its use as adsorbent. Alternatively, clays minerals have been widely used as adsorbents in the removal of phenol and Cr(VI) due to their low cost, high cations exchange capacity (CEC) and layered structure [12]. While in their natural forms, clays adsorb weakly due to their hydrophilic properties. These properties can be improved by the simple modification through the intercalation of the clay sheets by the conventional cationic surfactants to convert the clay surface from hydrophilic to hydrophobic character. The modification concerns the exchange of inorganic cations in their interlayer with organic cations such as quaternary ammonium cations. The resulting organoclays, using a range of surfactants have been widely used for organic and inorganic pollutants removal [13 - 20].

Consequently, in this work we have tested the efficiency of initially bentonite (Bt), and organically modified bentonite by Hexadecyltrimethylammonium bromide (HDTMABt) in the removal of phenol and chromium in separate solutions. Long chain (C > 12) quaternary ammonium modified bentonite has not been enough explored for chromium compared with those in relation to phenol. Moreover, the choice of these pollutants is based on the fact that in Morocco there are many industries for tanning leather and the production of olive's oil which reject a large amount of phenol and chromium exceeding the accepted standards.

XRD (X ray diffraction), FTIR (Fourier Transform Infrared Spectrometer), BET (Brunauer, Emmet and Teller) and SEM/EDX (scanning electron microscopy/energy dispersive X-ray) were used to characterize the samples. Fo any batch adsorption, the experimental data were fitted to various kinetics and isotherms equations. The thermodynamic parameters were also determined.

2. Materials and methods

2.1. Materials

The bentonite (Bt) was provided from Rhone Poulenc Company (France). HDTMABr [$(CH_3)_3NC_{16}H_{33}Br$], Potassium dichromate ($K_2Cr_2O_7$), $AgNO_3$ and phenol were purchased from Aldrich chemicals and specified to be ≥ 99% purity. Deionised water was used in all experiments. All other reagents such as HCl and NaOH were of analytical grade.

2.2. Preparation of HDTMABt composite

Prior to the HDTMABt preparation, the Bt was treated by NaCl to form sodium bentonite (NaBt). The NaBt was prepared by stirring a known weight of Bt in 200 ml of 10^{-1} mol/L NaCl solution during 24h at room temperature, then it was separated by centrifugation (15000 rpm) and washed several times until no Cl is was detected by $AgNO_3$ test. The composite HDTMABt was prepared by exchanging Na^+ in NaBt by $HDTMA^+$ cations as follows: a total amount of 30 g of NaBt was added to the known concentration of surfactant solution (HDTMABr: C(mol/L)) and stirred for 24 h with a mechanical stirrer at 25 °C. The composite was separated from the solution by centrifugation, and the excess of the surfactant was removed by repetitive washing with distilled water until no bromide ion was detected by $AgNO_3$ test. The obtained HDTMABt was dried in air at 60 °C, ground and stored until use.

2.3. Adsorption experiments

Initial stocks concentrations of 6.10^{-5}M – 8.10^{-3}M for phenol and chromium were prepared separately. A total of 0.1 g or 0.2 g of NaBt or HDTMABt were mixed with V = 20 mL of phenol or chromium solutions in erlenmeyer flasks with glass caps. The flasks were shaken for different times of adsorption (t_{ads}) at certain temperature (T_{ads}) on a shaker at 150 rpm. The pH solutions were adjusted by adding negligible volumes of 0.1 mol/L HCl or NaOH. After a given t_{ads}, the solid and liquid phases were separated by centrifugation at 15000 rpm. The residual concentration (C_r) of phenol or chromium in supernatant were measured by UV/Visible spectrophotometer (UV/Vis 2100 from Shimadzu) at λ = 270 nm and λ = 350 nm, respectively. The amount of phenol or chromium adsorbed at equilibrium on NaBt or HDTMABt was calculated using the following equation:

$$q_e = \left(\frac{C_0 - C_e}{m}\right).V \quad (1)$$

ISSN 2321-807X

Where C_0 and C_e were the initial and the equilibrium concentrations of pollutants (mg/L), respectively, m was the mass of adsorbent (g) and V the volume of the solution (L).

2.4. Characterizations of materials

Several spectroscopic techniques were used to characterize the NaBt and the HDTMABt: (a) XRD patterns were obtained using a X'PERT MPD-PRO wide angle X-ray powder diffractometer operating at 45 kV and 40 mA with CuKα radiation, (b) FTIR spectra were recorded in absorption frequencies (400 – 4000 cm^{-1}) in an FTIR (Shimadzu, JASCO 4100). The samples were prepared in KBr discs from very well dried mixtures of about 4% (w/w) and stored in a desiccator, (c) solid morphology was determined using SEM (Philips) supplied with EDX detector (Quantax 400) and (d) N_2 adsorption measurements at - 196 °C were performed using an ASAP 2010. The specific surface area and the average pore diameter were determined according to the standard BET and BJH (Barrett, Joyner and Halenda) methods, respectively.

3. RESULTS AND DISCUSSION

3.1. Characterization of the samples: NaBt and HDTMABt

The FTIR spectra of NaBt and its modified forms (HDTMABt) with various concentrations of HDTMABr (ranged from 10^{-4}M to 10^{-1}M) are presented in fig.1. It can be noticed that there is net difference between the original sample and the HDTMABt characterized by the appearance of new bands at 2850 cm^{-1} and 2920 cm^{-1} related to the symmetric and asymmetric CH_2 and CH_3 stretching vibration. Their two bending vibrations located at 1463 and 1474 cm^{-1}, due to the methylene scissoring modes, could be observed in FTIR spectra of $HDTMA^+$ and cetyltrimethylammonium bromide clays with relative higher concentration of surfactant [13,21,22]. The existence of the strong bands at 2850 cm^{-1} and 2920 cm^{-1} and their scissoring modes constitutes an evidence of $HDTMA^+$ intercalation in the interlayer space of NaBt. Their intensities increase as the concentration C of the surfactant increases and remains the same even at the highest surfactant loading level ($C \geq 5.10^{-2}$M), indicating the saturation of NaBt sites by the exchange reaction. The N–CH_3 stretching peak at 3016 cm^{-1}, appeared only after the addition of C(HDTMABr) ≥ 5.10^{-2}M has been attributed to the highest value of the cationic exchange capacity (CEC > 1), when the confined surfactant in the interlayer changed from lateral to paraffin arrangements with different tilting angles resembling more to HDTMABr solid [13,21,23,24]. In the OH region, between 3100 cm^{-1} and 3700 cm^{-1}, two bands can be distinguished at 3638 and 3456 cm^{-1} accompanied by a shoulder at 3220 cm^{-1}. The latter was attributed to the water hydrogen bonded to other water molecules within the interlayer [24,25]; whereas the first band at 3638 cm^{-1} was attributed to the inner OH unit within the clay structure. The position and intensity of the last band are not affected by $HDTMA^+$ loading on NaBt. It's also observed (fig.1) that when the concentration of $HDTMA^+$ increases up to 10^{-1}M, the position of the band at 3456 cm^{-1}, which was originated from adsorbed water, shifts to lower frequency from 3456 cm^{-1} to 3434 cm^{-1} accompanied with a decrease in their absorbance. The same trend was observed for the band at 1634 cm^{-1} and attributed to OH deformation vibration. The displacement of these bands can be linked to the exchange reactions occurring in the interlayer of NaBt. Similar results were reported by other authors using bentonite or other clays [13,17,25]. In their interpretations, they suggest the loss of the water of hydration as the cations (Na^+) are replaced by the cationic surfactant. These results indicate that the head groups of $HDTMA^+$ are attached to the aluminosilicate layer surface with a relatively high order at a higher $HDTMA^+$ loading.

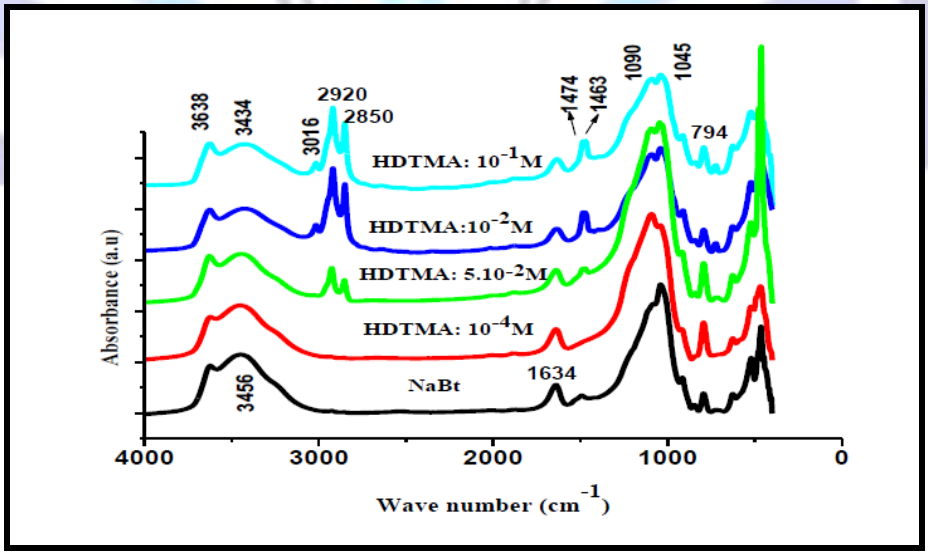

Fig 1: FTIR spectra of NaBt and HDTAMBt

ISSN 2321-807X

The characteristic bands in the region 900–1200 cm^{-1} were attributed to different types of Si–O and Si–O–Si stretching vibrations. Additional bands between 450 and 900 cm^{-1} in the spectrum of NaBt were assigned to typical Si–O and Si–O–Al bending modes [13, 26].

Finally, the FTIR results show that the saturation of NaBt by $HDTMA^+$ was obtained for $C \geq 5.10^{-2}M$. Consequently it can be noted that all the adsorption experiments were carried out with NaBt and HDTMABt ($C = 10^{-1}M$).

Other evidences for the intercalation of NaBt by $HDTMA^+$ were obtained by ESM/EDX, XRD and BET analyses. ESM (Fig.2) indicates that there are notable morphological differences between NaBt and the prepared HDTMABt. For NaBt (Fig.2a) porous texture with curled and crumpled structure is observed. These characteristics are not visible on the SEM micrographs of the HDTMABt sample with $HDTMA^+$ ($C = 10^{-1}M$) due to surfactant coverage on the external crystal surface (Fig.2b) confirming, thus, a good homogeneity within the organo-clays.

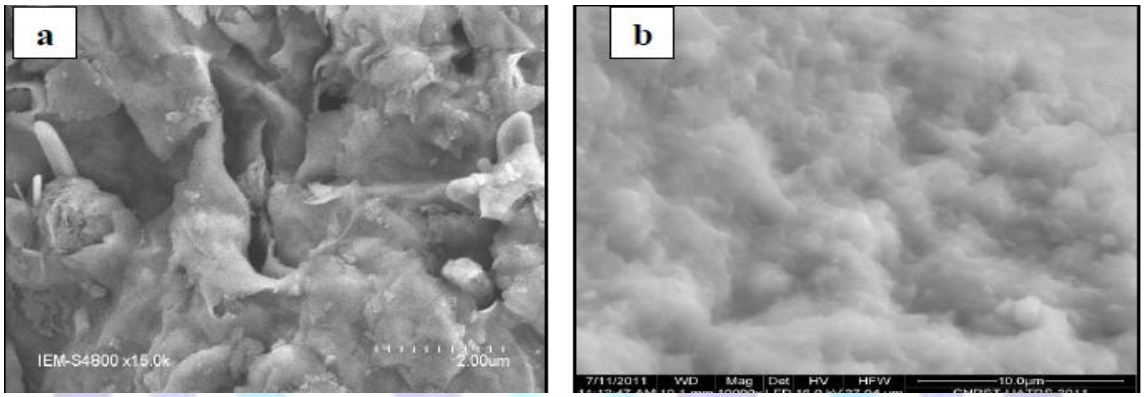

Fig 2: ESM micrographs of (a) NaBt and (b) HDTAMBt

The XRD patterns of NaBt and its organoclays are shown in figure.3. For NaBt, the basal spacing d(001) centered at d = 15.34 Å shifts to d = 19.32 Å in the HDTMABt indicating that the $HDTMA^+$ ($C = 10^{-1}M$) cations has been intercalated within the layered structure widened the basal spacing of NaBt. The new peaks appearing at 2θ° = 6.7 and 2θ° = 9 are the result of the regular stacking of surfactant alkyl chains on each other, reflecting the highest value of the CEC > 100% and the pseudotrimolecular layer (d ≈ 20-21 Å) arrangements as well as the monolayer and bilayer of paraffin type structures in the interlayers space of bentonite [12, 22, 23, 27].

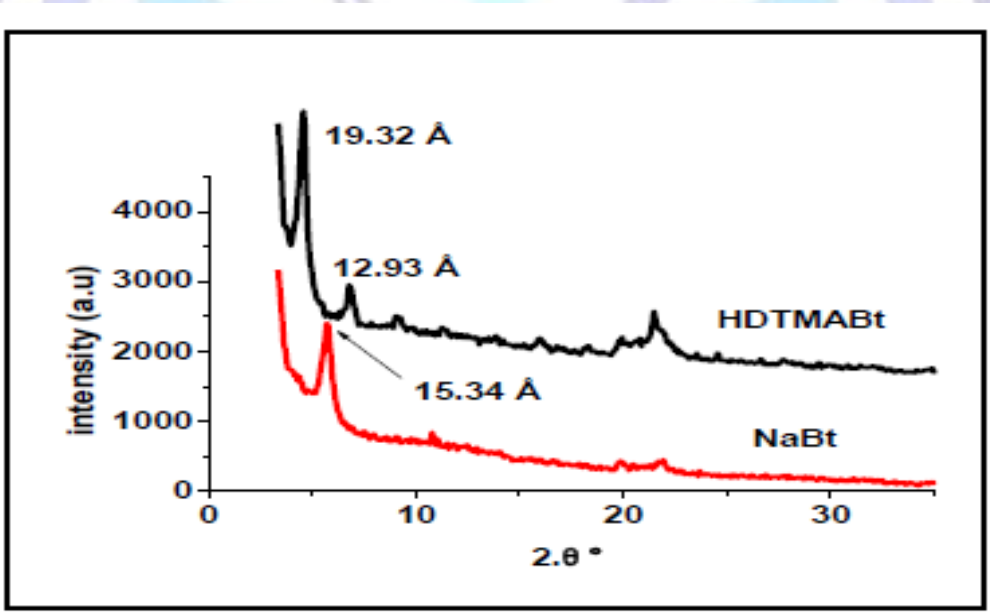

Fig 3: XRD paterns of the NaBt and HDTAMBt ($C = 10^{-1}M$)

ISSN 2321-807X

The above results explain the decrease in BET specific surface area and cumulative pore volume when NaBt is modified by $HDTMA^+$ and the increase of the average pore diameter (Table1). It was due to obstruction of mesopores by $HDTMA^+$ cations, thus, impeding the diffusion of N_2 throughout these channels. The obtained values were in good accordance with the conclusions cited in literature [14,16,22,28] which indicate that the significant decreases of the values of these parameters correspond to the high surfactant loadings in the interlayer space of NaBt.

Table 1. Structural parameters of NaBt and HDTMABt.

Samples	S_{BET} (m^2/g)	Vp: Total pore volume (cm^3/g)	dp:Average pore diameter (Å)
NaBt	19.43	0.0584	120.10
HDTMABt	2.04	0.0087	170.21

3.2. SORPTION KINETICS

3.2. 1. Effect of contact time

Kinetics of chromium and phenol adsorption were examined at pH = 2 and pH = 9 respectively, on both NaBt and HDTMABt adsorbents (Fig.4(a,b)). The results show that on all the studied samples the adsorption of chromium pollutant is very fast than that obtained for phenol. The maximum rate of removal occurred within t < 1 h of contact time thereafter, no change was observed which indicates that the system has reached the equilibrium point. It is also seen that the amounts of chromium and phenol adsorbed at equilibrium increased on modified bentonite independently of their specific surface area. It is clear that the presence of $HDTMA^+$ in the interlayer space promotes the adsorption ability of NaBt, possibly by offering additional sites for phenol and chromium uptake. The rapid uptake and the augmentation of the amounts adsorbed would be ideal for industrial application.

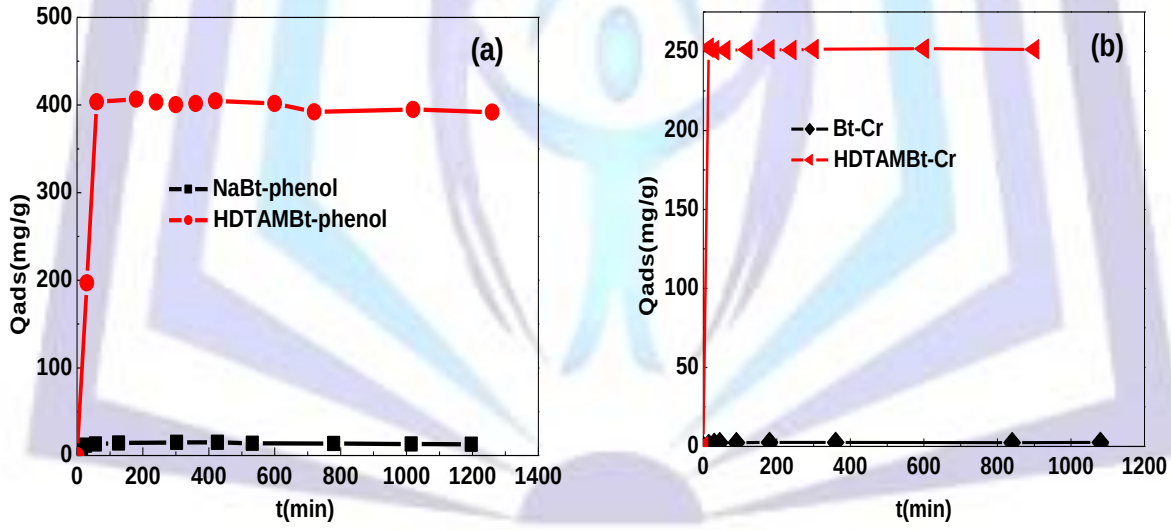

Fig 4: Relationship between phenol (a) and chromium (b) uptake and reaction time:

(C_{phenol} = 2.10^{-3}M), (C_{Cr} = 2.10^{-4}M) and T = 25°C

To elucidate the adsorption mechanism of phenol and chromium onto HDTMABt and NaBt, the experimental data were confronted to the pseudo-first-order and the pseudo-second-order kinetics models [29]. In this study, no correlation was found for the pseudo-first order model (not shown), while the linear form of the pseudo-second-order provided a best correlation (R^2 = 0.999) for the adsorption data of phenol and chromium onto NaBt and HDTMABt (Fig.5). The equation used is:

$$\frac{t}{q_t} = \frac{1}{(k_2 q_e^2)} + \frac{t}{q_e} \quad (2)$$

where q_e and q_t are the amount of pollutants (mg/g) at equilibrium and at various time t (min), respectively, and k_2 (g/mg/min) is the pseudo-second-order rate constant.

The values of k_2 and $q_{e,cal}$ were calculated from the intercepts and slopes of the linear plots of t/q_t vs. t (Fig.7) respectively, and are presented in table 2. It is observed that the values of $q_{e,cal}$ deduced from this model were close to the amounts obtained experimentally ($q_{e,exp}$) for both the considered pollutants. Therefore, the chemical sorption is the rate controlling step in the adsorption kinetic of phenol and chromium on NaBt and HDTMABt.

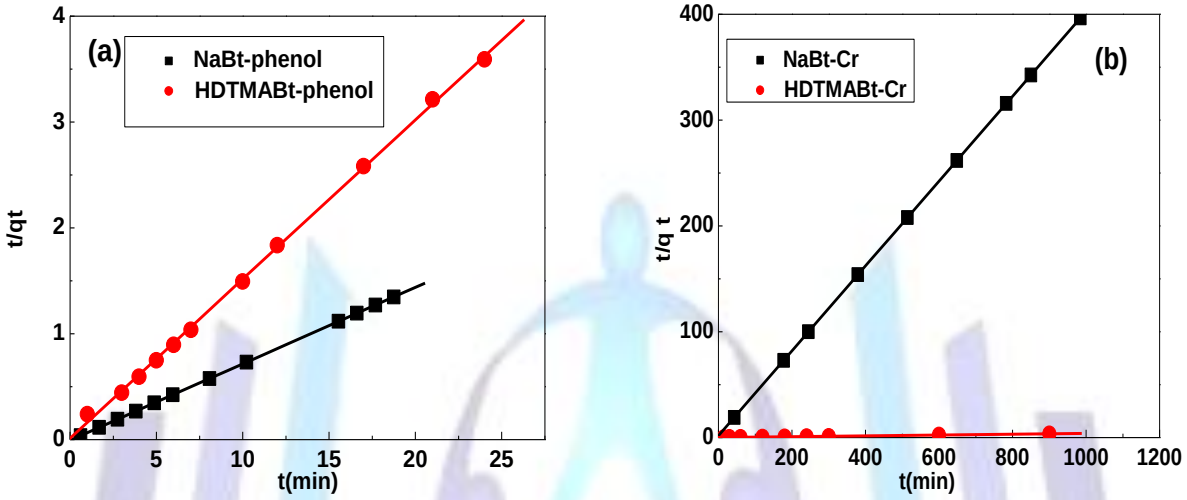

Fig 5: Pseudo-second-order kinetics of phenol (a) and chromium (b) at T_{ads} = 25 °C

Table 2. Parameters of kinetic adsorption model for phenol and chromium on NaBt and HDTMABt at T_{ads} = 25 °C.

	Samples	$q_{e,exp}$ (mg/g)	Pseudo-first-order			Pseudo-second-order		
			$q_{e,cal}$ (mg/g)	k_1 (min^{-1})	R^2	$q_{e,cal}$ (mg/g)	k_2 (g/mg.min)	R^2
Cr	NaBt	2.5	1.25	0,008	0.998	2.5	$8.65.10^{-2}$	0.999
	HDTMABt	251.7	5.75	4.10^{-5}	0.996	270.3	0.0060	0.999
Phenol	NaBt	14.5	16.55	0.081	0.846	13.7	0.0089	0.999
	HDTMABt	406	2.35	_	0.997	416.7	0.0015	0.999

3.2.2. Adsorption isotherms

In order to optimize the design of an adsorption system, it is important to establish the most appropriate correlation for the equilibrium data. The more common adsorption isotherm models of Langmuir and Freundlich were applied to fit the equilibrium data for the adsorption of Cr(VI) and phenol onto NaBt and HDTMABt. The linear forms of those models are expressed by the following equations:

$$\text{Langmuir : } q_e = \frac{q_m.K_L.C_e}{1+K_L.C_e} \quad (3) \qquad ; \qquad \text{Freundlich : } q_e = K_F.C_e^{\,1/n} \quad (4)$$

where q_e(mg/g) is the amount adsorbed per unit mass of adsorbent, Ce(mg/L) is the equilibrium concentration, q_m(mg/g) is the monolayer adsorption capacity, n is the adsorption intensity or surface heterogeneity, K_L(L/mmol) and K_F(mg/g) are the sorption affinity constant relates the heat of adsorption and the adsorption capacity, respectively.

Values of Langmuir and Freundlich constants are calculated from the intercept and slope of the plots (Fig.6(a,b)), and are listed in table 3. It is obvious from figure 6a that the applicability of the linear equation of Langmuir model is not adequate with the data of the experimental isotherm obtained for the adsorption of phenol onto NaBt and HDTMABt, while in the case of chromium, the experimental data were well fitted (fig.6b), indicating that both Langmuir and Freundlich

ISSN 2321-807X

isotherm models can describe the adsorption of this pollutant onto the two samples. Similar results have been reported by other authors for the adsorption of phenol and chromium by unmodified and organo-modified bentonite [2,3,12,16,27]. The increase in K_F values of the adsorbent corresponds to more active sites while the decrease in 1/n may be regarded as increased surface heterogeneity in modified NaBt, and all the values determined for 1/n were less than unity (0 < 1/n < 1), indicating favourable adsorption.

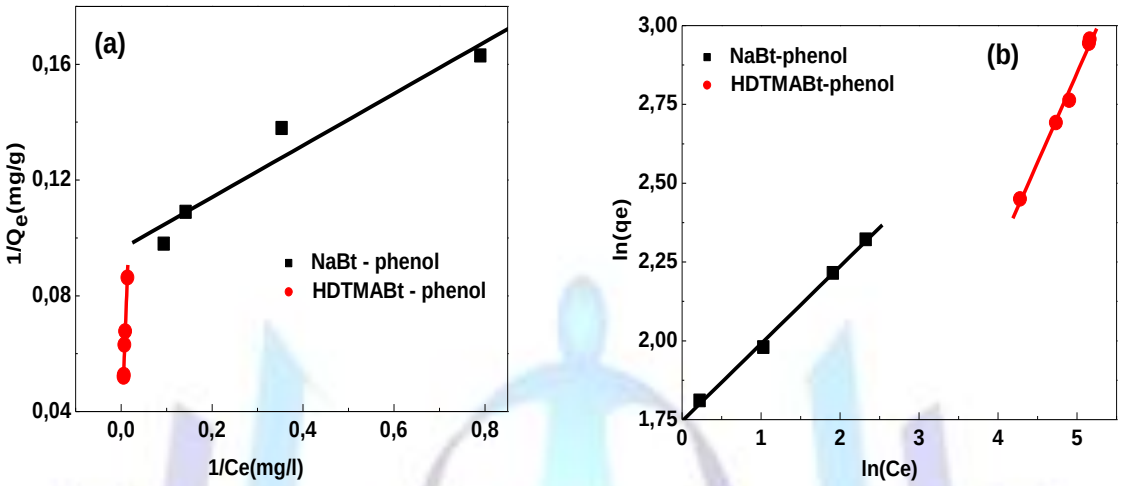

Fig 6a: Langmuir (a) and Freundlich (b) plots for the adsorption of phenol at T_{ads} = 25 °C.

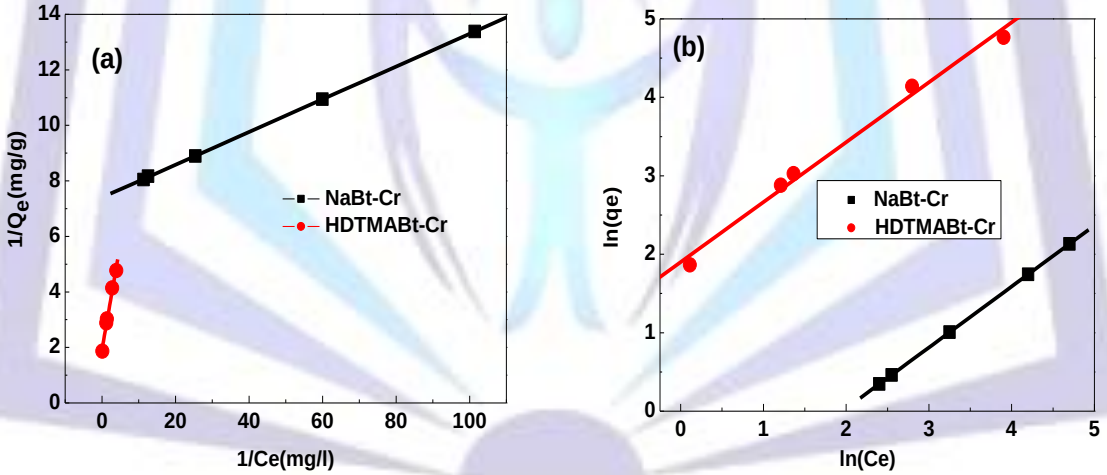

Fig 6b: Langmuir (a) and Freundlich (b) plots for the adsorption of chromium at T_{ads} = 25°C

ISSN 2321-807X

Table 3. Model parameters for the sorption of phenol and chromium on NaBt and HDTMABt.

	Chromium				Phenol			
	NaBt		HDTMABt		NaBt		HDTMABt	
	Langmuir	Freundlich	Langmuir	Freundlich	Langmuir	Freundlich	Langmuir	Freundlich
q_{max} (mg/g)	16,950	-	250	-	10,980	-	34,480	-
K_L	8.10^{-3}	-	0,024	-	0,940	-	0,007	-
R_L	0,415	-	0,414	-	-	-	0,883	-
R^2	0,990	0,99	0,990	0,990	0,936	0,990	0,980	0,990
K_F	-	0,22	-	6,685	-	5, 640	-	1,008
1/n	-	0,78	-	0,763	-	0,246	-	0,568

In order to understand the difference between the observed adsorption data, obtained for chromium and phenol, it is important to take into account the experimental conditions applied for each pollutant especially, the pH value and the arrangements of surfactants in the organo-bentonite which influences strongly the adsorption onto the solid/liquid interface:

- Chromium (VI):

Some researchers [30-32] have recently shown in their evaluation of modified mineral performance for chromium sorption from aqueous solutions that the high adsorption capacity of $HDTMA^+$-clay has shown a maximum at pH = 3-4 and has been linked to the adsorption of predominate $HCrO_4^-$ and $Cr_2O_7^{2-}$ species of Cr(VI) which require one exchange site for each anion in order to be adsorbed. The exchanges reaction was referred to the exchange of bromide or chloride ions from HDTMA/Br or HDTMA/Cl adsorbed on the intercalated NaBt. This mechanism can be accepted when the halide ions exist in the organoclay sample after its preparation. In this study, the samples were washed several times with distilled water until the supernatant solution was free of bromide (test of $AgNO_3$). Thus, at pH = 2 the negatively charged chromium species interact with the $HDTMA^+$ cations which reverse the surface charge of NaBt and enhances, therefore, the adsorption of chromium species. This may be due to electrostatic attraction forces working between the organoclay and $HCrO_4^-$ and $Cr_2O_7^{2-}$ species, in good agreement with other propositions [3,30 - 33]. In addition, at low pH value, more adsorption might be due to increase in number of protons on orgaoclay which in turn neutralizes the negatively charged hydroxyl group (OH^-) on adsorbed surface, thereby, reducing the hindrance to the diffusion of Cr(VI) ions into the interlayer space of organoclay. Kumar et al. [19], indicate the contribution of the OH_2^+ groups in the clay to the enhancement of chromium adsorption by surface complexation with $HCrO_4^-$ species. Majdan et al. [32], observed an 11.5 Å increase in d(001) basal spacing value on the SWAXS (Small wide angle X-ray scattering measurements) pattern recorded before and after adsorption of chromium. This shifts was attributed to the presence of dichromates $(HDTMA)_2Cr_2O_7$ and chromates $(HDTMA)(HCrO_4)$ in the interlayer space of HDTMA-bentonite. For XRD pattern of chitosan clay composite, the new peaks observed after adsorption of Cr(VI) at pH = 3 and the shifts of d(001) to lower 2θ°, were linked to the adsorbed Cr(VI) onto the silicate surface and also in the lamellar space of the cloisite 10 Å [34]. The interaction of Cr(VI) with (OH) and $HDTMA^+$ groups were also confirmed by the infrared spectrum of HDTMABt-Cr [19,35].

- Phenol:

The pH applied was 9, and the results showed that the removal of phenol by HDTMABt seems to be more effective than unmodified sample. The differences in the adsorption capacity can be explained by the difference in the affinity between phenol and surfactant cations. Thus, for phenol pKa ≈ 9.95, and at pH = 9, the phenol is mainly in molecular form or in the form of phenolates ($C_6H_5O^-$). The latter is more polar and the attractive force between quaternary ammonium cations and polar molecules is weaker than that between these cations and non-polar molecules [17]. Other works [36,37] reported that the reduction in adsorption of phenol on clay at pH > 8 was due to the abundance of OH^- ions which increased hindrance to diffusion of phenol ions and electrostatic repulsion between the negatively charged surface sites of the sorbent and phenolic ions. On the positively charged surface of HDTMABt, the OH^- can act as competing or inhibitor ions to phenolate anions, thus, the effect of repellency between the ionized phenol and the negative particle was enhanced in high pH region. Regarding the results obtained, the sorption efficiency towards phenol seems to mainly depend on the presence of $HDTMA^+$ in the interlayer space of NaBt rather than S_{BET}, Vp and pore diameter. XRD studies concluded that the adsorption of phenol leads probably to the exfoliation of the interlayer through hydrophobic interaction and, at the same time, to the disturbance of the arrangements of intercalated $HDTMA^+$ chains [36]. As reported [22,27], the adsorbed phenol has a significant effect on the arrangement of the intercalated $HDTMA^+$ or other surfactants. They concluded that the sorption mechanism can include partition of organic compounds into hydrophobic phase created by surfactant loaded of organoclay, adsorption basis of the sorbents and also adsorption on the external space of the clay. Majdan et al.[27], observed a change from 17.93 to 19.38 Å with the phenol concentration increasing from $2.1.10^{-5}$ to $3.26.10^{-3}$ mol/g, and suggested that the phenol molecule adopts predominantly the flat position in relation to the lateral bilayer of $HDTMA^+$ cations, or is directed at a small angle to the surface of structural layers.

4. CONCLUSIONS

The intercalation of $HDTMA^+$ cations within the interlayer space were confirmed using various useful techniques. The experiments showed that the organoclay with higher surfactant concentration ($C=10^{-1}M$) was more effective in removing phenol and chromium species pollutants than the original NaBt exchanged bentonite. The maximum phenol and chromium uptakes were achieved at pH = 9 and pH = 2, respectively. The kinetic studies indicated that the adsorption process was extremely fast on HDTMABt, and the sorption system fitted well with pseudo-second order for both pollutants. For the adsorption of phenol, Freundlich isotherm gave the best fit, and this indicated that the adsorption system is likely to involve multilayer sorption, while for chromium the experimental isotherms were best described by Freundlich and Langmuir models. The adsorption mechanism may be through hydrophobic interaction between $HDTMA^+$ and the pollutants (partitioning affinities), or by their intercalation in the interlayer space as evidenced for phenol. The results of this study indicate that HDTMABt was an effective sorbent for both chromium and phenol solutes which are usually present in waste water. Additional research is needed to evaluate the adsorption efficiency of organoclay using real wastewater.

ACKNOWLEDGMENTS

The authors appreciate the financial support given through the University of My Ismail project ((Project UMI 2011).

REFERENCES

[1] Aksu, Z., G¨onen,F., 2012. Separation and Purification Technology 49, 205–216.

[2] Khezami, L., Capart, R., 2005. Journal of Hazardous Materials B123, 223–231.

[3] Gładysz-Plaska, A., Majdan, M., Pikus, S., Sternik, D., 2012. Chemical Engineering Journal 179, 140-150.

[4] Busca, G., Berardinelli, S., Resini, C. Arrighi, L., 2008. Journal of Hazardous Materials 160, 265-288.

[5] O'Connell, D.W., Birkinshaw, C., O'Dwyer, T.F., 2008. Bioresource Technology 99, 6709–6724.

[6] Ahmaruzzaman, M., 2008. Advances in Colloid and Interface Science 143, 48–67.

[7] Bhatnagar, A., Sillanpaa, M., 2010. Chemical Engineering Journal 157, 277–296.

[8] Lin, S.H., Juang, R.S., 2009. Journal of Environmental management 90, 1336-1349.

[9] Hernández-Montoya,V. Pérez-Cruz, M.A., Mendoza-Castillo, D.I., Moreno-Virgen, M.R., Bonilla-Petriciolet A., 2013. Journal of Environmental Management 116, 213-221.

[10] Saha, B., Orvig, C., 2010. Coordination Chemistry Reviews 254, 2959–2972.

[11] Zhang, Z., Zhang, Z., Fernandez, Y., Menendez, J.A., Niu, H., Peng, J., Zhang, L., Guo, S., 2010. Applied Surface Science 256 (2010) 2569–2576.

[12] Sarkar, B., Xia,Y., Megharaj,M., Krishnamurtia, G.S.R., Rajarathnam, D., Naidu, B., 2010. Journal of Hazardous Materials 183, 87–97.

[13] Li, Z., Jiang, W.T., Hong, H., 2008. Spectrochimica Acta Part A 71, 1525–1534.

[14] Park, Y., Ayoko, G.A., Kurdi,R., Ho,E., Horvath b, Kristof, J., b, Frost, R.L., 2013. Journal of Colloid and Interface Science 406, 196–208.

[15] Wang, C., Jiang, X., Zhou, L., Xia, G., Chen, Z., Duan, M., Jiang, X., 2013. Chemical Engineering Journal 219, 469–477.

[16] Mirmohamadsadeghi, S., Kaghazchi, T., Soleimani, M., Asasian, N., 2012. Applied Clay Science 59–60, 8–12.

[17] Nguyen,V.N., Nguyen, T.D.C, Dao, T.P., Tran, H.T., Nguyen, D.B., Ahn,D.H., 2013. Journal of Industrial and Engineering Chemistry 19, 640–644.

[18] Alkaram, U.F., Mukhlis, A.A., Al-Dujaili. A.H., 2009. Journal of Hazardous Materials 169, 324–332.

[19] Kumar, A.S.K., Ramachandran, R., Kalidhasan, S., Rajesh, V., Rajeshet, N., 2012. Chemical Engineering Journal, 211-212, 396-405.

[20] Lee, Y.C., Park, W.K., Yang, J.W., 2011. Journal of Hazardous Materials 190, 652–658.

[21] Hongping, H., Ray, F.L., Jianxi, Z., 2004. Spectrochimica Acta Part A 60, 2853–2859.

[22] Zhou, Q., He, H.P., Zhu, J.X., Shen,W., Frost, R.L., Yuan, P., 2008. Journal of Hazardous Materials 154, 1025–1032.

[23] Zhu, J., He, H., Zhu, L., Wen, X., Deng, F., 2005. Journal of Colloid and Interface Science 286, 239–244.

[24] Zhou, Q., Frost, R.L., He, H., Xi, Y., Liu, H., 2007. Journal of Colloid and Interface Science 307, 357–363.

[25] Xue, W., He, H., Zhu, J., Yuan, P., 2007. Spectrochimica Acta Part A 67, 1030–1036.

[26] Hrachová. J, Madejová. J, Billik. P, Komadel. P, Fajnor, V. Š., 2007. Journal of Colloid and Interface Science 316, 589–595.

[27] Majdan, M., Sabah, E., Bujacka, M., Pikus, S., Płaska, A.G., 2009. Journal of Molecular Structure 938, 29–34.

[28] Su, J., Lin, H.F., Wang, Q.P., Xie, Z.M., Chen. Z.L., 2011. Desalination 269, 163–169.

[29] Ho, Y.S., McKay, G., 1999. Process Biochemistry 34, 451-465.

[30] Hu, B., Luo, H., Chen, H., Dong, T., 2011. Applied Clay Science 51, 198–201.

[31] Thanos, A.G., Katsou, E., Malamis, S., Psarras, K., Pavlatou, E.A., Haralambous, K.J., 2012. Chemical Engineering Journal 211–212, 77–88.

[32] Majdan, M., Maryuk, O., Pikus, S., Olszewska, E., Kwiatkowski, R., Skrzypek, H., 2005. Journal of Molecular Structure 740, 203–211.

[33] Dultz, S., An, J.H., Riebe, B., 2012. Applied Clay Science 67–68 (2012) 125–133.

[34] Pandey, S., Mishra, S.B., 2011. Journal of Colloid and Interface Science 361, 509–520.

[35] Hong, H., Jiang, W.T., Zhang, X., Tie, L., Li, Z., 2008. Applied Clay Science 42, 292–299.

[36] Nayak, P.S., Singh, B.K., 2007. Desalination 207, 71–79.